

See discussions, stats, and author profiles for this publication at: <https://www.researchgate.net/publication/245368608>

Stream-of-Variation (SOVA) Modeling—Part II: A Generic 3D Variation Model for Rigid Body Assembly in Multistation Assembly Processes

Article in *Journal of Manufacturing Science and Engineering* · August 2007

DOI: 10.1115/1.2738953

CITATIONS

135

READS

716

4 authors, including:



Wenzhen Huang

University of Massachusetts Dartmouth

31 PUBLICATIONS 1,012 CITATIONS

[SEE PROFILE](#)



Zhenyu James Kong

Virginia Tech (Virginia Polytechnic Institute and State University)

131 PUBLICATIONS 2,741 CITATIONS

[SEE PROFILE](#)

Some of the authors of this publication are also working on these related projects:



Geometric Integrity in Additive Manufacturing [View project](#)



'2mm' Program [View project](#)

Wenzhen Huang
Department of Mechanical Engineering,
University of Massachusetts,
Dartmouth, MA 02747
e-mail: whuang@umassd.edu

Jijun Lin
Engineering Systems Division,
School of Engineering,
Massachusetts Institute of Technology,
Cambridge, MA 02139-4307
e-mail: jijunlin@mit.edu

Zhenyu Kong
School of Industrial Engineering and
Management,
Oklahoma State University,
Stillwater, OK 74078
e-mail: james.kong@okstate.edu

Dariusz Ceglarek
Dept. of Industrial and Systems Engineering,
University of Wisconsin-Madison,
Madison, WI 53706
e-mail: darek@engr.wisc.edu

Stream-of-Variation (SOVA) Modeling—Part II: A Generic 3D Variation Model for Rigid Body Assembly in Multistation Assembly Processes

A 3D rigid assembly modeling technique is developed for stream of variation analysis (SOVA) in multi-station processes. An assembly process is modeled as a spatial indexed state transition dynamic system. The model takes into account product and process factors such as: part-to-fixture, part-to-part, and inter-station interactions, which represent the influences coming from both tooling errors and part errors. The incorporation of the virtual fixture concept (Huang et al., Proc. of 2006 ASME MSEC) and inter-station interaction leads to the generic, unified SOVA model formulation. An automatic model generation technique is also developed for surmounting difficulties in modeling based on first principles. It enhances the applicability in modeling complex assemblies. The developed SOVA methodology outperforms the current simulation based techniques in computation efficiency, not only in forward analysis of complex assembly systems (tolerance analysis, sensitivity analysis), but it is also more powerful in backward analysis (tolerance synthesis and dimensional fault diagnosis). The model is validated using industrial case studies and series of simulations conducted using standardized industrial software (3DCS Analyst). [DOI: 10.1115/1.2738953]

1 Introduction

1.1 Problem Description. Multi-station assembly processes generally refer to the processes involving multiple work-stations to manufacture a complex assembly. For example, an automotive body assembly process, consisting of up to 70 stations and several hundreds of sheet panels, is a typical multi-station assembly process to fabricate the body-in-white of an automobile.

Dimensional quality, represented by product dimension variability, is one of the most critical challenges in industries such as automotive, aerospace, shipbuilding, appliance, etc. The scale and complexity of the multistage manufacturing systems (MMS) in these industries greatly increase the difficulties in modeling, analysis, and control of dimensional variation in both design and manufacturing phases. Lack of modeling tools has pushed the problems downstream (e.g., ramp-up and launch), which can incur a huge amount of cost. For example, two-thirds of engineering changes in automotive and aerospace industries are caused by dimensional faults [1].

The overall importance of dimensional variation in manufacturing processes is also reflected by extensive research focused on dimensional variation modeling, faults diagnosis, and tolerance design [2–15,28]. Statistical analysis of variation propagation in multi-station assembly processes is important to quality and productivity improvement. The complexity of a manufacturing process puts high demands on process modeling, design optimization, and fault diagnosis to ensure the dimensional integrity of products.

There are two main error sources in an assembly system: fixture locating error and part error. In general, the variation propagation in rigid body assemblies is driven by three fundamental mecha-

nisms: (1) part-to-part interaction, (2) part-to-fixture interaction, and (3) inter-station interactions, which is in fact a specific type of (2) between stations. In Type I assembly, there is only part-to-part interaction, whereas for Type II assembly, both (1) and (2) interactions exist. They have been identified by industry as the two most frequent causes of engineering changes [16]. Inter-station interaction has been identified as one of the contributors in multi-station assembly processes [17].

Efforts have been made in SOVA modeling in multi-station assembly processes. A state space model was initially introduced for variation propagation in [18,19] and was recently developed in [4,6,28] for 2D assembly systems. More recently, an effort has been made to take into account both tooling and part errors in the 3D single station SOVA model [14]. Therefore, further efforts are desirable to provide a complete 3D SOVA model for multi-station assembly systems.

1.2 Related Work. The assembly modeling and variation control of multi-station manufacturing processes have become an emerging area on the boundaries of engineering and statistics research and have grown rapidly since its inception in the early 1990s.

Earlier research primarily preoccupied with statistical descriptions of variation patterns from in-line measurement data [2] or rule-based fault isolation method [20]. These diagnostic methods are primarily heuristic knowledge based. Engineering model-based diagnostics of fixture fault in the manufacturing process was initiated in [1] on the assumptions of single fault, single fixture, and rigid part. From then on, subsequent efforts have been made on more general assumptions, such as multiple faults, compliant components, and multiple fixtures [3,8,17,21,22,27].

Data driven techniques were developed in parallel for diagnosis. Lawless and co-workers [23–25] used an autoregressive (AR) model to investigate dimensional variation in assembly processes as well as in machining processes. They identify interrelations between their statistical model and the physical process by esti-

Contributed by the Manufacturing Engineering Division of ASME for publication in the JOURNAL OF MANUFACTURING SCIENCE AND ENGINEERING. Manuscript received August 14, 2006; final manuscript received March 27, 2007. Review conducted by Shivakumar Raman.

Table 1 Related work on state space modeling of multi-station assembly

	Mantripragada and Whitney [19]	Jin and Shi [18]	Ding, Ceglarek, and Shi [4]	Proposed 3D SOVA
Fixture error	No	Yes	Yes	Yes
Part manufacturing error	Yes	No	No	Yes
2D/3D	N/A	2D	2D	2D and 3D

imating the parameters of the AR model from real process measurements. The amount of variation attributable to different stages of a process is then studied to identify opportunities for variation reduction. Huang and Ceglarek [9,10] developed statistical modal analysis techniques for form error pattern identification and diagnosis in stamped parts.

The aforementioned research activities have significantly advanced process monitoring and diagnosis for dimensional control of assembly processes. However, lack of models describing the overall assembly process has imposed a significant constraint on the capability of variation prediction and root cause diagnosis in design and manufacturing.

As such, efforts have already been initiated in the last decade to characterize variation propagation in multi-station assembly processes. Jin and Shi [18] introduced a state space model (SSM) for variation modeling; a spatial indexed model and observation equation were established. In a similar vein, [19] employed a state transition model to describe the propagation of variation in assembly processes. The quality state was defined as kinematical deviations of parts in an assembly, which were produced from variation factors at each station and transmitted through the system. These models took advantage of the well-established techniques in modern control theory for design analysis, monitoring, and diagnosis. Ding et al. [4] developed a 2D SSM for modeling multistage sheet metal assembly processes. The associated assumptions include: (1) rigid part, (2) 3-2-1 fixture locating scheme, (3) in-plane deviation (2D), (4) fixture locator errors, and (5) lap joint. This model adopted the concepts and methods from control theory and used rigid 2D kinematics to establish linear models with explicit design parameters. The linear explicit SSM model has the advantages of highly efficient computation, model transparency (clear physical explanation), and incorporation of sensing information for diagnosis. These developments provided a unified framework for both *forward analysis* (e.g., sensitivity and tolerance analysis) and *backward analysis* (e.g., synthesis and diagnosis). A comprehensive review of 2D SSM modeling techniques was given in [6] and summarized in Table 1.

In spite of these developments, the numerical simulation based method for variation analysis of rigid body assembly has already been developed and used in commercialized variation analysis software such as 3DCS. The focus is on forward design simulation and tolerance analysis. Numerical algorithms and Monte Carlo (MC) simulation are the major tools for the calculation. Major concerns of the MC based techniques are the tedious computation and tremendous processing time required, in particular, in complex high-dimensional design synthesis and diagnosis problems. Efforts have also been made for improvement. [11,26] introduced number-theoretical net quasi-MC which can improve the computation efficiency of MC based techniques in tolerance design problems.

To improve the model generality and applicability of current SSM, it is desirable to develop models on more general assumptions. More recently, Huang and co-workers [10,14] developed a single station SOVA model for 3D rigid part assembly. Fixture/part errors and different types of joints are taken into account in the model. A concept of generalized *virtual fixture* was created to formulate variation caused by part mating errors and fixture errors in a unified framework. This work provided an infrastructure for further expansion of single station SOVA model to a generic 3D SOVA model in multi-station systems.

1.3 Objective and Organization. This paper aims at developing a variation propagation model for 3D rigid part assembly.

This 3D SOVA model provides a linear analytical tool for system evaluation and synthesis, thus going beyond the current 2D SOVA model and numerical simulation techniques. To achieve model generality and applicability, the model should be able to: (1) include part and fixture error sources, (2) take into account different types of joints, (3) formulate 3D variation propagation in multi-stations, and (4) be implemented easily. Since the model is directly derived from first principles, it tends to be too complicated and thus impractical for complex assemblies in application. Another focus of this paper is, therefore, on an efficient model generation method.

This paper is organized into six sections. Section 2 starts with assumptions used in the paper, and then identifies and formulates variation factors in a multi-station assembly process. In Sec. 3.1, we initially introduce three theorems for modeling error accumulation, whereby the 3D SOVA model is developed in Secs. 3.2–3.4. An automatic SOVA model generation method is developed in Sec. 3.5. In Sec. 4, a simulation example, as well as a floor-pan and a truck cab assembly as examples from the automotive industry are presented for model validation. The conclusion is given in Sec. 5.

2 Assumptions and Variation Factors

The underlying assumptions are initially introduced; the variation factors within a station and between stations are then formulated. Three main contributors of product dimensional variation are formulated in this section.

2.1 Assumptions. The assumptions are introduced below:

- Rigid assembly, i.e., all parts are taken as a rigid body in the assembling process; therefore, part deviation can be represented by any specified reference point (RP);
- Rigid mating interface, i.e., the mating plane error is modeled as a plane undergoing a rigid body movement from its nominal position;
- Fixture errors and part errors;
- 3-2-1 fixture locating scheme, the *generalized fixture* concept in [14] is used when a part or a subassembly is positioned by both fixture and part mating interface;
- Four typical joint types: lap joint, butt joint, mixed joint, and T joint;
- Small errors (compared with part and assembly dimensions).

The first four assumptions have been widely accepted in the literature and in the industrial variation control practices [1–4,18–20]. The rigid assumption is valid for the open assembly, which does not produce a structural closure with lock-in stresses [12]. A complete assembly model involves both rigid and compliant components (i.e., hybrid model) and requires more comprehensive assumptions such as the *n*-2-1 locating scheme and part compliancy, which is beyond the scope of this paper. Although part mating features are confined to the typical joint types in sheet metal panel assembly, the more general types of joints in mechanical assemblies can actually be modeled by using the techniques introduced in [10,14]. The small error assumption is intro-

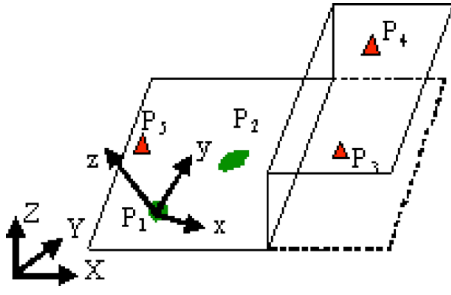


Fig. 1 Generic 3-2-1 fixture layout in GCS

duced for model linearization. The fixture and part dimensional errors are usually two to three orders smaller than the part dimensions.

2.2 Station-Level Variation Factors. At station level there are two major variation sources: **fixture imperfection** and **part manufacturing imperfection**. Fixture imperfection leads to part positioning error or deviation in an assembly. Manufacturing imperfection refers to dimensional or geometrical errors, generated on part mating features in part fabricating processes. To model the stream of variation in a single station, a method has been developed in [14] that integrated these error sources in a unified format with a *generalized (virtual) fixture* concept. **The deviation of a part in an assembly is represented in the global coordinate system (GCS), whereas fixture and part errors are represented in the local coordinate system (LCS).** In the modeling process, the effects of fixture errors and part errors are formulated and transformations of parts deviations between GCS and LCS are introduced.

2.2.1 Fixture Error. We consider a generic fixture locating scheme in Fig. 1 that represents a 3-2-1 locating scheme in a GCS. In this section, we will provide the relationship between the fixture error in LCS and RP deviation in the GCS. The variation flow through part-part interfaces and fixtures can be unitedly formu-

lated with a “*generalized fixture*” or “*virtual fixture*” as shown in [14]; therefore, the fixture model provides a fundamental basis in the multi-station SOVA modeling.

Denote the errors on locators P_1 – P_5 in the LCS as

$$\Delta f = (\Delta x_1, \Delta y_1, \Delta x_2, \Delta y_2, \Delta z_3, \Delta z_4, \Delta z_5)^T \quad (1)$$

The xyz LCS centers at the four-way pin P_1 . Let us define a primary plane orthogonal to the four-way pin P_1 's orientation as direction z . The normal vector of this primary plane is denoted as $Z(n_x, n_y, n_z)$, which is expressed in XYZ GCS. Three in-plane degrees of freedom (displacements in x and y directions and rotation around the z axis) are fully controlled by P_1 and P_2 . The other three degrees of freedom (translation in z direction, rotation about x , and y axes) are controlled by locators P_3 – P_5 .

Given the normal vector of primary plane: $z(n_x, n_y, n_z)$ in XYZ GCS. Local x and y axes in the primary plane can be determined by

$$z = n_x \mathbf{i} + n_y \mathbf{j} + n_z \mathbf{k} \quad (2)$$

$$\mathbf{x} = \mathbf{Z} \times \mathbf{z} = -n_y \mathbf{i} - n_x \mathbf{j} \quad (3)$$

$$\mathbf{y} = \mathbf{z} \times \mathbf{x} = -n_x n_z \mathbf{i} - n_y n_z \mathbf{j} + (n_y^2 - n_x^2) \mathbf{k} \quad (4)$$

For any LCS with direction cosines of x , y , and z as l^i, m^i , and $n^i, i \in \{x, y, z\}$ in a GCS, the coordinate transformation matrix Φ is given in [10,14]. Using the results in Eqs. (2)–(4)

$$\Phi = \begin{bmatrix} l^x & m^x & n^x \\ l^y & m^y & n^y \\ l^z & m^z & n^z \end{bmatrix} = \begin{bmatrix} -n_y & -n_x & 0 \\ -n_x n_z & -n_y n_z & (n_y^2 - n_x^2) \\ n_x & n_y & n_z \end{bmatrix} \quad (5)$$

Denote a deviation on a part by ΔP_r on any specified RP, we have [14]

$$\Delta P_r^{\text{global}} = \begin{bmatrix} \Phi & 0_{3 \times 3} \\ 0_{3 \times 3} & \Phi \end{bmatrix}^{-1} \Delta P_r^{\text{local}} = \bar{\Phi}^{-1} \Delta P_r^{\text{local}} \quad (6)$$

ΔP_r caused by fixture error in LCS can be derived in [10]

$$\Delta P_r^{\text{local}} = \begin{Bmatrix} \Delta P_p \\ \Delta P_o \end{Bmatrix} = \{\Delta x, \Delta y, \Delta z, \Delta \alpha, \Delta \beta, \Delta \gamma\}_r = F_s \Delta f \quad (7)$$

$$= \begin{bmatrix} 1 & 0 & 0 & 0 & 0 & 0 & 0 \\ 0 & 1 & 0 & 0 & 0 & 0 & 0 \\ 0 & 0 & 0 & 0 & D_{35} & D_{36} & D_{37} \\ 0 & 0 & 0 & 0 & D_{45} & D_{46} & D_{47} \\ 0 & 0 & 0 & 0 & D_{55} & D_{56} & D_{57} \\ \frac{\sin \lambda}{L} & -\frac{\cos \lambda}{L} & -\frac{\sin \lambda}{L} & \frac{\cos \lambda}{L} & 0 & 0 & 0 \end{bmatrix} \begin{Bmatrix} \Delta x_1 \\ \Delta y_1 \\ \Delta x_2 \\ \Delta y_2 \\ \Delta z_3 \\ \Delta z_4 \\ \Delta z_5 \end{Bmatrix}_{\text{local}} \quad (8)$$

where, L is the length of projection vector $\mathbf{P}_1 \mathbf{P}_2$ in primary plane. λ is the angle between x axis and $\mathbf{P}_1 \mathbf{P}_2$ in primary plane. D_{ij} can be derived with P_1 – P_5 coordinates [10]. In the F_s matrix there is no element associated with z components of P_1 – P_5 . Thus, we can first project P_1 – P_5 onto the primary plane, and then construct the F_s matrix based on x and y coordinates of P_1 – P_5 :

$$\bar{F}_s = \begin{bmatrix} \Phi & 0_{3 \times 3} \\ 0_{3 \times 3} & \Phi \end{bmatrix}^{-1} F_s \quad (9)$$

Therefore, using Eqs. (6)–(9) we have

$$\Delta P_r^{\text{global}} = \bar{F}_s \Delta f^{\text{local}} \quad (10)$$

Obviously \bar{F}_s , and $\bar{\Phi}$ are **fixture specific**. If a part is fully constrained by a fixture, Eq. (10) provides the relationship of the **fixture error and part deviation**. It can be extended to the part being constrained by a fixture and mating features [10,14].

2.2.2 Part Manufacturing Imperfection. If part $k-1$ is assembled with the deviation $\Delta P_{r(k-1)}$ in GCS. When part k is joining in through part $k-1$, the deviation ΔP_{rk} will be caused by upstream deviation $\Delta P_{r(k-1)}$, mating feature errors between $k-1$

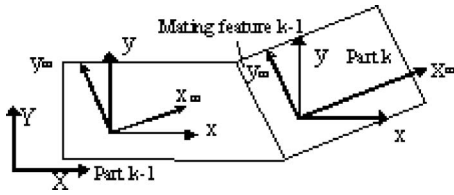


Fig. 2 Coordinate transformation between mating planes

and k , and fixture errors on part k .

In [14], the mating features, which partially constrain a part in an assembly, have been formulated in a *generalized fixture*. The locally defined mating feature errors have a similar effect on parts positioning, as presented in Sec. 2.2.1. To accommodate arbitrary position and orientation of mating feature planes with respect to GCS, we define a LCS on each mating feature plane. The transformations for $\Delta P_{r(k-1)}$ and ΔP_{rk} between GCS and LCS are first introduced (Fig. 2). The superscript “ m ” on part deviations represents it is in mating feature LCS. Then the error stack up from part $k-1$ to part k is formulated.

There are three sequential steps for coordinate transformations and error stack formulation as illustrated below:

- (1) $\Delta P_{r(k-1)}$ in GCS $\rightarrow \Delta P_{r(k-1)}^m$ in LCS
- (2) $\Delta P_{r(k-1)}^m$ in LCS $\rightarrow \Delta P_{rk}^m$ in LCS
- (3) ΔP_{rk}^m in LCS $\rightarrow \Delta P_{rk}$ in GCS

Steps 1 and 3 are GCS and LCS coordinates transformations. Based on Eq. (7), the deviation of RP expressed in two coordinate systems is

$$\Delta P_r^m = \bar{\Phi} \Delta P_r^{\text{global}} \quad (11)$$

Applying Eq. (7) to part $k-1$ and part k , respectively, it yields

$$\Delta P_{r(k-1)}^m = \bar{\Phi}_{k-1} \Delta P_{r(k-1)} \quad \Delta P_{rk} = \bar{\Phi}_{k-1}^{-1} \Delta P_{rk}^m \quad (12)$$

Step 2 formulates the error stack-up process. According to the theory in [14], the deviation of a RP on part k is determined by:

- (1) The deviation of the RP on part $k-1$, i.e., $\Delta P_{r(k-1)}$,
- (2) Local mating transformation: $\bar{\Phi}_{(k-1)}$,
- (3) The errors of mating feature plane $k-1$ (between part k and part $k-1$), i.e., $\Delta \Omega_{b(k-1)}$ and $\Delta \Omega_{ak}$,
- (4) Fixture error on part k , i.e., Δf_k .

Considering all these four factors, the error propagation through mating feature can be expressed as

$$\Delta P_{rk} = J_{k-1} [\Delta P_{r(k-1)}', \Delta \Omega_{b(k-1)}', \Delta \Omega_{ak}', \Delta f_k']^T \quad (13)$$

where

$$J_i = \bar{\Phi}_i^{-1} \bar{J}_i \begin{bmatrix} \bar{\Phi}_i & 0 \\ 0 & I \end{bmatrix}_{25 \times 25} \quad (14)$$

$$\bar{J}_i = \begin{cases} \bar{B}_i & \text{The } i\text{th joint is a butt joint} \\ \bar{L}_i & \text{The } i\text{th joint is a lap joint} \\ \bar{M}_i & \text{The } i\text{th joint is a mixed joint} \\ \bar{T}_i & \text{The } i\text{th joint is a T joint} \end{cases} \quad (15)$$

where \bar{B}_i , \bar{L}_i , \bar{M}_i , and \bar{T}_i are joint-specific matrices defined in [10,14].

2.3 Reorientation-Induced Variation. Shiu et al. [17] revealed the reorientation phenomenon in the multi-station process.

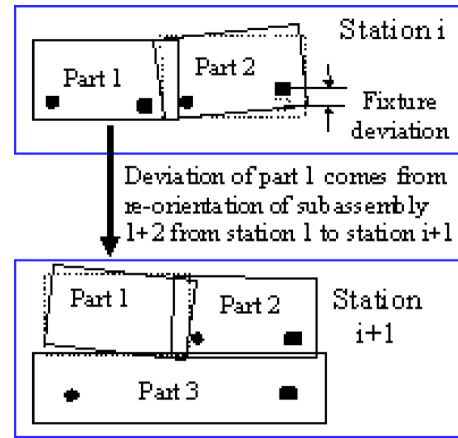


Fig. 3 Deviation from reorientation

The reorientation is defined as repositioning due to transferring subassemblies between stations that consist of different data schemes. For example, after part 1 and part 2 are joined together at station i , the subassembly is transferred to station $i+1$ (Fig. 3). If only pin-holes on part 2 are used to position the subassembly “1+2” at station $i+1$, part 1 deviates from its nominal position even if fixtures are perfect at station $i+1$. This station-station transition induced deviation is defined as the reorientation error. The dashed line represents the nominal positions of parts, while the solid line indicates the actual positions.

We consider the deviation accumulation of part J in the assembly process at the i th station. In a similar vein as in 2D assembly systems [4,18,28], the state vector (deviation) $\mathbf{X}^J(i)$ of an assembly at station i comes from $\mathbf{X}^J(i-1)$, fixture and mating feature error-induced deviation \mathbf{E}_1^J , and reorientation-induced deviation \mathbf{E}_2^J ; that is,

$$\mathbf{X}^J(i) = \mathbf{X}^J(i-1) + \mathbf{E}_1^J(i) + \mathbf{E}_2^J(i) \quad (16)$$

Equation (16) is illustrated in Fig. 4. Two deviation terms, \mathbf{E}_1^J and \mathbf{E}_2^J in Eq. (16), are given by the following Lemmas.

Case 1. If part J is first merged into the assembly stream as a single part in station i , we can use the single station assembly model to calculate $\mathbf{E}_1^J(i)$. The reorientation error $\mathbf{E}_2^J(i)$ is zero.

Case 2. Suppose part J is already in subassembly $s(i-1)$ and it is joined into the main assembly in station i along with a root subassembly, which is fully constrained by a fixture. The accumulated deviation can thus be expressed as

$$\Delta P_r^J(i) = \Delta P_r^J(i-1) + \mathbf{E}_1^J(i) + \mathbf{E}_2^J(i) \quad (17)$$

where \mathbf{E}_1^J is caused by fixture error of $P_{s1(i)} - P_{s5(i)}$; \mathbf{E}_2^J is due to subassembly error of $P_{s1(i)}(i-1) - P_{s5(i)}(i-1)$. All terms in Eq. (17) are expressed in GCS. \mathbf{E}_1^J and \mathbf{E}_2^J are given by the following Lemmas 1 and 2.

Lemma 1. Suppose part J transits with subassembly s from

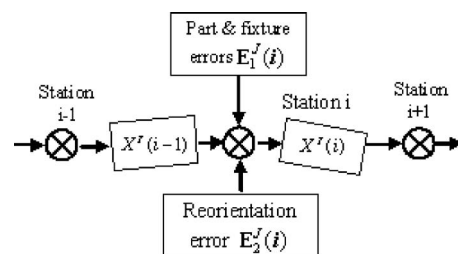


Fig. 4 Deviation accumulation on part J at station i

station $i-1$ to i , the fixture error-induced deviation $\mathbf{E}_1^J(i)$ is

$$\mathbf{E}_1^J(i) = \bar{\mathbf{Q}}(P_{s1}(i), P_r^J) \mathbf{E}_{1s}(i) \quad (18)$$

where $\mathbf{E}_{1s}(i)$ is the RP deviation on subassembly $s(i)$. Let us choose P_{s1} as RP. From Eq. (10), it yields

$$\mathbf{E}_{1s}(i) = \bar{F}_{s(i)} \Delta f_{s(i)} \quad (19)$$

and

$$\mathbf{E}_{1s}(i) = (\Delta x_{rs(i)}, \Delta y_{rs(i)}, \Delta z_{rs(i)}, \Delta \alpha_{rs(i)}, \Delta \beta_{rs(i)}, \Delta \gamma_{rs(i)})' \quad (20)$$

$$\Delta f_{s(i)} = (\Delta x_{P_{s1}}, \Delta y_{P_{s1}}, \Delta x_{P_{s2}}, \Delta y_{P_{s2}}, \Delta z_{P_{s3}}, \Delta z_{P_{s4}}, \Delta z_{P_{s5}})' \quad (21)$$

$\Delta f_{s(i)}$ is the fixture error expressed in the local coordinate system of subassembly $s(i)$, and $\bar{F}_{s(i)}$ is defined in Eq. (9). The transformation between the deviations of any two points in the same part can be expressed as [10,14]

$$\mathbf{E}_1^J(i) = \bar{\mathbf{Q}}(P_{s1}(i), P_r^J) \mathbf{E}_{1s}(i) \quad (22)$$

$$\bar{\mathbf{Q}}(P_{s1}(i), P_r^J) = \begin{bmatrix} I_{3 \times 3} & Q(P_{s1}(i), P_r^J) \\ 0 & I_{3 \times 3} \end{bmatrix} \quad (23)$$

$$Q(P_{s1}(i), P_r^J) = \begin{bmatrix} 0 & z & -y \\ -z & 0 & x \\ y & -x & 0 \end{bmatrix} \quad (24)$$

In the matrix $Q(P_{s1}(i), P_r^J)$, we express P_r^J in the local coordinate system which centers at $P_{s1}(i)$ and has parallel axes to global coordinate axes. If there are k_{i-1} parts in subassembly $s(i)$, the deviation of all RPs due to subassembly $s(i)$ fixture error can be expressed as

$$\mathbf{E}_1^{s(i)}(i) = [\mathbf{E}_1^1(i), \mathbf{E}_1^2(i), \dots, \mathbf{E}_1^{k_{i-1}}(i)]^T \quad (25)$$

or $\mathbf{E}_1^{s(i)}(i) = \mathbf{M}(P_{s1}(i), P_r) \mathbf{E}_{1s}(i)$.

Substituting Eq. (22) into Eq. (25) yields

$$\mathbf{E}_1^{s(i)}(i) = \mathbf{M}(P_{s1}(i), P_r) \bar{F}_{s(i)} \Delta f_{s(i)} \quad (26)$$

$$\mathbf{M}(P_{s1}(i), P_r) = \begin{bmatrix} \bar{\mathbf{Q}}(P_{s1}(i), P_r^1) \\ \bar{\mathbf{Q}}(P_{s1}(i), P_r^2) \\ \vdots \\ \bar{\mathbf{Q}}(P_{s1}(i), P_r^{k_{i-1}}) \end{bmatrix} \quad (27)$$

The Lemma 2 below characterizes the motion of transferring parts between stations. Suppose a subassembly $s(i-1)$ be positioned by $P_{s1}(i)-P_{s5}(i)$ at station i , if there is no fixture deviation at the current station i but there is deviation accumulated in $P_{s1}(i)-P_{s5}(i)$ at the previous station $i-1$, then the subassembly undergoes rotation and translation when moving from station $i-1$ to station i .

Lemma 2. $\mathbf{E}_2^J(i)$ at station i is caused by the deviation of locating points accumulated up to station $i-1$, therefore,

$$\mathbf{E}_2^J(i) = \bar{\mathbf{Q}}(P_{s1}(i), P_r^J) \mathbf{E}_{2s}(i) \quad (28)$$

The translation and rotation of subassembly $s(i-1)$ when moving from station $i-1$ to station i can be expressed as a linear combination of deviation accumulated in its locating points $P_{s1}(i)-P_{s5}(i)$ at the previous station $i-1$. Thus, $\mathbf{E}_{2s}(i)$ can be expressed as

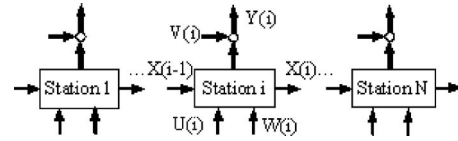


Fig. 5 An assembly process with N stations

$$\mathbf{E}_{2s}(i) = -\bar{F}_{s(i)} [\Delta x_{\rho_1}, \Delta y_{\rho_1}, \Delta x_{\rho_2}, \Delta y_{\rho_2}, \Delta z_{\rho_3}, \Delta z_{\rho_4}, \Delta z_{\rho_5}]^T = -\bar{F}_{s(i)} \Delta_L \quad (29)$$

Here, $\rho_k = P_{sk(i)}(i-1)$, $\Delta X_{P_{s1}(i)}(i-1) - \Delta Z_{P_{s5}(i)}(i-1)$ are deviations of the locating points $P_{s1}(i)-P_{s5}(i)$ at the previous station $i-1$, and they could be in different parts. As in Lemma 1 the same transformations can be used for calculating the accumulated deviation of $\Delta X_{P_{s1}(i)}(i-1) - \Delta Z_{P_{s5}(i)}(i-1)$. If there are k_{i-1} parts in subassembly $s(i)$, the deviation of all RPs due to reorientation of subassembly $s(i-1)$ is

$$\mathbf{E}_2^{s(i)}(i) = [\mathbf{E}_2^1(i), \mathbf{E}_2^2(i), \dots, \mathbf{E}_2^{k_{i-1}}(i)]^T \quad (30)$$

which can be written as

$$\mathbf{E}_2^{s(i)}(i) = \mathbf{M}[P_{s1}(i), P_r] \mathbf{E}_{2s}(i) \quad (31)$$

where $\mathbf{M}(P_{s1}(i), P_r)$ is defined in Eq. (27).

3 State Space Model for 3D Assembly in MMS

To improve the generality and applicability, in this section, the 2D state space model [4,19,28] is generalized and extended for 3D assembly in multi-station processes. The same framework is adopted with modification in model matrices for incorporation of fixture/part errors and 3D geometric factors.

The stream of variation in an MMS is illustrated in Fig. 5 for an N -station process; all the vectors are defined below. $x(i) \in R^{n \times 1}$ is the accumulated deviation; $U(i) \in R^{m(i) \times 1}$ is the fixture/part deviation contributed from station i ; $Y(i) \in R^{q(i) \times 1}$ is the measurement obtained on station i ; superscripts n , $m(i)$, $q(i)$ are dimensions of the three vectors, respectively; $W(i)$, $V(i)$ are mutually independent noise.

The stream of variation in this MMP is characterized by the following equations:

$$X(i) = A(i-1)X(i-1) + B(i)P(i) + W(i) \quad i = 1, 2, \dots, N \quad (32)$$

$$Y(i) = C(i)X(i) + V(i) \quad \{i\} \subset \{1, 2, \dots, N\} \quad (33)$$

where the first equation, the state equation, implies that part deviation on station i is influenced by two sources: the accumulated variation up to station $i-1$ and the variation contribution on station i ; the second equation is the observation equation. Detailed expressions of system matrices $A(i)$, $B(i)$, and $C(i)$ will be derived in this section.

3.1 Theorems. Suppose there are k_{i-1} parts assembled together from upstream processes. They form a subassembly $s(i)$ in station $i-1$, and we add $k_i - k_{i-1}$ parts sequentially to subassembly $s(i)$ at station i . At the end of station i , there are k_i parts in the subassembly/product. Therefore, the state vector $X(i)$ is updated station by station, which is shown in Eq. (32)

$$X(i) = [X^1(i), \dots, X^{k_{i-1}}(i) | X^{k_{i-1}+1}(i), \dots, X^{k_i}(i) | X^{k_i+1}(i), \dots, X^{n_i}(i)]^T \quad (34)$$

where n_i is the total number of parts in final product.

In the following discussion, we will introduce two theorems and then derivate the system matrices $A(i-1)$, $B(i)$, and $C(i)$ in Eq. (32).

THEOREM 1. Suppose in the station i there are totally k_{i-1} parts in root subassembly $s(i)$, the reorientation-induced error $E_2^{s(i)}(i)$ for the subassembly $s(i)$ can be expressed as

$$E_2^{s(i)}(i) = -\mathbf{M}(P_{s1}(i), P_r) \bar{F}_{s(i)} G(i) \begin{bmatrix} X^1(i-1) \\ X^2(i-1) \\ \vdots \\ X^{k_{i-1}}(i-1) \end{bmatrix} \quad (35)$$

where

$$G(i) = F_2 Q(i) S(i) \quad (36)$$

$$F_2 = [f_{ij}]_{7 \times 15} \text{ with } f_{11} = f_{22} = f_{34} = f_{45} = f_{59} = f_{6,12} = f_{7,15} = 1, \text{ otherwise, } f_{ij} = 0 \quad (37)$$

$$Q(i) = \text{diag}\{Q_i\} \quad i = 1-5 \quad (38)$$

$$Q_i = [I_{3 \times 3} \quad \tilde{Q}_i] \quad i = 1-5 \quad (39)$$

$$\tilde{Q}_i = \begin{bmatrix} 0 & z & -y \\ -z & 0 & x \\ y & -x & 0 \end{bmatrix} \quad (40)$$

$(x, y, z)_i$, $i = 1-5$ is the P_1-P_5 coordinates in the root subassembly's local coordinate system.

$S(i)$ is a selecting matrix, which selects parts that have locators in root subassembly at station i :

$$S(i) = [\delta_{ij} I_{6 \times 6}]_{30 \times 6k_{i-1}} \quad i = 1, \dots, 5, j = 1, \dots, k_{i-1} \quad (41)$$

Suppose the root subassembly's locators P_1-P_5 belong to parts $a, b, c, d, e \in (1, k_{i-1})$, respectively:

$$\delta_{1m} = \begin{cases} 1 & \text{if } m = a \\ 0 & \text{if } m \neq a \end{cases} \quad \delta_{2m} = \begin{cases} 1 & \text{if } m = b \\ 0 & \text{if } m \neq b \end{cases}$$

$$\delta_{3m} = \begin{cases} 1 & \text{if } m = c \\ 0 & \text{if } m \neq c \end{cases} \quad \delta_{4m} = \begin{cases} 1 & \text{if } m = d \\ 0 & \text{if } m \neq d \end{cases}$$

$$\delta_{5m} = \begin{cases} 1 & \text{if } m = e \\ 0 & \text{if } m \neq e \end{cases}$$

Proof. Comparing Lemma 2, Eqs. (29) and (31) with Eq. (36), we only need to prove

$$\Delta_L = G(i) [X^1(i-1), X^2(i-1), \dots, X^{k_{i-1}}(i-1)]^T \quad (42)$$

The proof is very straightforward. From Eq. (36), $G(i) = F_2 Q(i) S(i)$. The $S(i)$ matrix selects RP deviation of the parts, which have five locating points P_1-P_5 . $Q(i)$ further translates the deviation of this RP error to locating points' error accumulated up to station $s(i)$. Finally, the F_2 matrix selects the necessary component of the deviation.

THEOREM 2. Suppose in the station i there are k_{i-1} parts in root subassembly $s(i)$, and after applying reorientation- and fixture error-induced deviation, the new state vector of part $1-k_{i-1}$ becomes

$$\begin{bmatrix} X^1(i) \\ \vdots \\ X^{k_{i-1}}(i) \end{bmatrix} = M_{s(i)}(i) \begin{bmatrix} X^1(i-1) \\ X^2(i-1) \\ \vdots \\ X^{k_{i-1}}(i-1) \end{bmatrix} + M[P_{s1}(i), P_r] \bar{F}_{s(i)} \Delta f_{s(i)} \quad (43)$$

where

$$M_{s(i)}(i) = [I - M(P_{s1}(i)), P_r] \bar{F}_{s(i)} G(i) F_1(i) \quad (44)$$

$$F_1(i) = [I_{6k_{i-1} \times 6k_{i-1}} \quad 0_{6k_{i-1} \times 6(n_r - k_{i-1})}]_{6k_{i-1} \times 6n_r} \quad (45)$$

Proof. We can express Eq. (16) as a system vector equation for subassembly $s(i)$:

$$\begin{bmatrix} X^1(i) \\ \vdots \\ X^{k_{i-1}}(i) \end{bmatrix} = \begin{bmatrix} X^1(i-1) \\ \vdots \\ X^{k_{i-1}}(i-1) \end{bmatrix} + E_2^{s(i)}(i) + E_1^{s(i)}(i) \quad (46)$$

Substituting Eqs. (26) and (35) into Eq. (46) yields

$$\begin{bmatrix} X^1(i) \\ \vdots \\ X^{k_{i-1}}(i) \end{bmatrix} = (I - T(i)G(i))F_1(i) \begin{bmatrix} X^1(i-1) \\ \vdots \\ X^{k_{i-1}}(i-1) \end{bmatrix} + T(i)\Delta f_{s(i)} \quad (47)$$

where $T(i) = M(P_{s1}(i), P_r) \bar{F}_{s(i)}$. With the definitions in Eqs. (44) and (45), Eq. (43) can be obtained. In Eq. (43), the first term is the accumulated error of subassembly $s(i)$ after reorientation but before applying any fixture error to subassembly in station i , which is determined by state vector of station $i-1$.

THEOREM 3. Suppose in the station i there are totally k_{i-1} parts in root subassembly $s(i)$, and we add $k_i - k_{i-1}$ parts sequential to the subassembly $s(i)$ in the station i , the propagation of reorientation-induced error to downstream parts $k_{i-1}+1 \sim k_i$ can be expressed as

$$\bar{E}_2^{s(i)}(i) = \begin{bmatrix} {}^R X^{k_{i-1}+1}(i) \\ {}^R X^{k_{i-1}+2}(i) \\ \vdots \\ {}^R X^{k_i}(i) \end{bmatrix} = R(i-1) \begin{bmatrix} X^1(i-1) \\ X^2(i-1) \\ \vdots \\ X^{k_{i-1}}(i-1) \end{bmatrix} \quad (48)$$

where the superscript "R" means the reorientation-induced deviation component for state vector:

$$R(i-1) = H(i-1)F_3(i)M_{s(i)}(i) \quad (49)$$

$$F_3(i) = [0_{6 \times 6(k_{i-1}-1)} \quad I_{6 \times 6}]_{6 \times 6k_{i-1}} \quad (50)$$

$$H(i-1) = \begin{bmatrix} \tilde{J}_{k_{i-1}} \\ \tilde{J}_{k_{i-1}+1} \tilde{J}_{k_{i-1}} \\ \vdots \\ \tilde{J}_{k_{i-1}-1} \cdots \tilde{J}_{k_{i-1}} \end{bmatrix}_{6(k_i - k_{i-1}) \times 6} \quad (51)$$

$$\tilde{J}_j = J_j F_4 \quad (52)$$

where J_i is defined in Eq. (14). F_4 is defined as

$$F_4 = [I_{6 \times 6}, 0_{6 \times 6}, 0_{6 \times 6}, 0_{6 \times 7}]^T \quad (53)$$

Proof. Selecting matrix $F_3(i)$ selects deviation of the part k_{i-1} 's RP after reorientation. $H(i-1)$ calculates how the part k_{i-1} 's

deviation affects downstream assembling through part-to-part joints. According to Eq. (13), $\Delta\Omega_{b(k-1)}$, $\Delta\Omega_{ak}$, and Δf_k are all set to zero, because the $\bar{E}_2^{s(i)}(i)$ term only considers how part k_{i-1} 's RP deviation propagates through joints.

3.2 State Equation

3.2.1 $A(i-1)$

$$A(i-1) = \begin{cases} 0_{6n_i \times 6n_i} & \text{if } i = 1 \\ \begin{bmatrix} M_{s(i)}(i) & 0_{6(n_i-k_{i-1}) \times 6n_i} \end{bmatrix}_{6n_i \times 6n_i} + \begin{bmatrix} 0_{6k_{i-1} \times 6n_i} \\ R(i-1) \\ 0_{6(n_i-k_i) \times 6n_i} \end{bmatrix}_{6n_i \times 6n_i} & \text{if } i > 1 \end{cases} \quad (54)$$

$A(i-1)$ depends on locating schemes in processes. At the first station, the part deviation error due to the previous station is zero. Thus, for $i=1$, $A(0)=0_{6n_i \times 6n_i}$. If $i > 1$, $A(i-1)$ represents the error accumulation of RPs and changing of locating scheme. $M_{s(i)}(i)$ and $A(i-1)$ are defined in Theorem 1 and Theorem 3.

3.2.2 $B(i)$ and $U(i)$. Define the input error vector as

$$U(i) = \begin{cases} \left\{ \overbrace{\Delta f'_1, \Delta\Omega'_{b1}, \Delta\Omega'_{a2}, \Delta f'_2, \Delta\Omega'_{b2}, \dots, \Omega'_{ak_1}, \Delta f'_{k_1}, \Delta\Omega'_{bk_1}}^{\text{part } 1, \text{ part } 2, \dots, \text{part } k_1} \right\} & \text{if } i = 1 \\ \left\{ \overbrace{\Delta f'_{s(i-1)}, \Delta\Omega'_{s(i-1)}, \Delta\Omega'_{a(k_{i-1}+1)}, \Delta f'_{k_{i-1}+1}, \Delta\Omega'_{b(k_{i-1}+1)}, \dots, \Omega'_{ak_i}, \Delta f'_{k_i}, \Delta\Omega'_{bk_i}}^{\text{subassembly } s(i-1), \text{ part } k_{i-1}+1, \dots, \text{part } k_i} \right\} & \text{if } i > 1 \end{cases} \quad (55)$$

$$B(i) = \begin{cases} \Lambda(i)_{6n_i \times m(i)} & \text{if } i = 1 \\ \begin{bmatrix} M(P_{s1}(i), P_r) \bar{W}_0 \\ \Lambda(i) \end{bmatrix}_{6n_i \times m(i)} & \text{if } i > 1 \end{cases} \quad (56)$$

where

$$\Lambda(i) = \begin{cases} [\bar{W}_0, J_1 \bar{W}_1, \dots, J_{k_i-1} \bar{W}_{k_i-1} | 0_{6(n_i-k_{i-1}) \times m(i)}]' & \text{if } i = 1 \\ [J_{k_{i-1}} \bar{W}_1, J_{k_{i-1}+1} \bar{W}_2, \dots, J_{k_i-1} \bar{W}_{k_i-1} | 0_{6(n_i-k_{i-1}) \times m(i)}]' & \text{if } i > 1 \end{cases} \quad (57)$$

where J_i is given in Eq. (14) as \bar{J}_i .

$$m(i) = \begin{cases} 19k_i - 6 & \text{if } i = 1 \\ 19(k_i - k_{i-1} + 1) - 6 & \text{if } i > 1 \end{cases} \quad (58)$$

and

$$\bar{W}_0 = [\bar{F}_{s(i)} | 0 \cdots 0]_{6 \times m(i)}$$

$$\bar{W}_0 = F_3(i) M(P_{s(i)}, P_r) W_0$$

$$\bar{W}_1 = \begin{bmatrix} \bar{W}_0 \\ U_0 \end{bmatrix}_{25 \times m(i)} \quad U_0 = [0_{19 \times 7} | I_{19 \times 19} | 0 \cdots 0]_{19 \times m(i)}$$

$$\bar{W}_2 = \begin{bmatrix} \bar{J}_{k_{i-1}} \bar{W}_1 \\ U_1 \end{bmatrix}_{25 \times m(i)} \quad U_1 = [0_{19 \times (7+19)} | I_{19 \times 19} | 0 \cdots 0]_{19 \times m(i)}$$

$$\begin{aligned} \bar{W}_3 &= \begin{bmatrix} \bar{J}_{k_{i-1}+1} \bar{W}_2 \\ U_2 \end{bmatrix}_{25 \times m(i)} \\ &= [0_{19 \times (7+2 \times 19)} | I_{19 \times 19} | 0 \cdots 0]_{19 \times m(i)} \end{aligned}$$

$$\bar{W}_j = \begin{bmatrix} \bar{J}_{k_{i-1}+j-2} \bar{W}_{j-1} \\ U_{j-1} \end{bmatrix}_{25 \times m(i)}$$

$$U_{j-1} = [0_{19 \times (7+(j-1) \times 19)} | I_{19 \times 19} | 0 \cdots 0]_{19 \times m(i)} \quad (59)$$

where \bar{W}_0 selects the deviation of parts K_{i-1} 's RP point, which is the starting point for error accumulation in station i .

3.3 Observation Equation. If sensors are put along the assembly line, the observation equation could be obtained. If there are r^J measurement points on part J at station i , then the deviation of each point on part J is

$$y_{\xi}^J(i) = \bar{Q}(P_r^J, \text{MLP}_{\xi}^J) X^J(i) \quad \xi = 1, 2, \dots, r^J \quad (60)$$

where

$$\bar{Q}(P_r^J, \text{MLP}_{\xi}^J) = \begin{bmatrix} I_{3 \times 3} & Q(P_r^J, \text{MLP}_{\xi}^J) \\ 0 & I_{3 \times 3} \end{bmatrix} \quad (61)$$

$Q(P_r^J, \text{MLP}_{\xi}^J)$ is defined in Eq. (24) wherein (x, y, z) is in the local coordinate system, which centers at P_r^J and has parallel axes with respect to global coordinate axes. Thus, the measurement vector of part J is

$$Y^J(i) = [y_1^J(i), y_2^J(i), \dots, y_{r^J}^J(i)]_{6r^J \times 6}^T \quad (62)$$

which can be written as $Y^J(i) = C^J(i)X^J(i)$, where

$$C^J(i) = [\bar{Q}'(P_r^J, \text{MLP}_1^J), \dots, \bar{Q}'(P_r^J, \text{MLP}_{r^J}^J)]_{6r^J \times 6}^T \quad (63)$$

Then, the deviation vector of all the measurement points is

$$Y(i) = [Y^1(i)^T, Y^2(i)^T, \dots, Y^{n_t}(i)^T]_{(6\sum_{j=1}^{n_t} r^j) \times 1}^T = C(i)X(i) \quad (64)$$

where $C(i)$ is a diagonal matrix of submatrices $C^k(i)$, i.e.

$$C(i) = \text{diag}\{C^k(i)\}, k = 1, \dots, n_t \quad (65)$$

If we consider noises $W(i)$ and $V(i)$, the complete model for deviation propagation is expressed in Eqs. (32) and (33).

3.4 Variation Propagation Model. The state space model of a multistage assembly process is represented in Eqs. (32) and (33), which take the same form as in 2D SSM. **Therefore, a similar procedure as in 2D SSM [4] can be adopted.** Suppose there is only end-of-line observation; that is, $i=N$ in Eq. (33). Adopting the state transition matrix $\Phi(\cdot, \cdot)$ from control theory, the input-output relationship can be represented as

$$Y = \sum_{i=1}^N C\Phi(N, i)B(i)U(i) + C\Phi(N, 0)X(0) + \varepsilon \quad (66)$$

where the state transition matrix is

$$\Phi(N, i) = A(N-1)A(N-2) \cdots A(i) \text{ and } \Phi(i, i) = I \quad (67)$$

$X(0)$ is the initial condition, resulted from manufacturing imperfection of stamped parts, and ε is the summation of all modeling uncertainty and sensor noise terms

$$\varepsilon = \sum_{i=1}^N C\Phi(N, i)W(i) + V \quad (68)$$

Define: $\gamma(i) = C\Phi(N, i)B(i)$ and $\gamma(0) = C\Phi(N, 0)$; then Eq. (68) can be simplified as

$$Y = \sum_{i=1}^N \gamma(i)U(i) + \gamma(0)X(0) + \varepsilon \quad (69)$$

Considering that $U(i)$ is a sequence of uncorrelated Gaussian random vectors with zero mean, the input-output variance relationship can be obtained from Eq. (66) as

$$\Sigma_Y = \sum_{i=1}^N \gamma(i)\Sigma_p(i)\gamma^T(i) + \gamma(0)\Sigma_0\gamma^T(0) + \Sigma_\varepsilon \quad (70)$$

where Σ represents the covariance matrix of a random vector (r.v.), that is

$$\Sigma_x = E\{[x - E(x)] [x - E(x)]^T\} \quad \forall \text{ r.v. } x \quad (71)$$

and Σ_0 is given as initial conditions.

The uncertainty term ε can be estimated from process tolerances, sensor specifications, and/or through historic data. So can

the covariance matrix Σ_0 of initial condition, which can be obtained based on incoming inspection. **The system can then be approximated with a pure linear relationship** as

$$\Sigma_Y = \sum_{i=1}^N \gamma(i)\Sigma_p(i)\gamma^T(i) \quad (72)$$

which indicates the variation of final product is contributed from variation of stamped part (input from precedent process) and variations of fixture errors at all stations.

3.5 Automatic SOVA Model Generation. The SSM SOVA model is appealing in both forward and backward applications for variation control in multi-station manufacturing processes. **However, direct derivation of the SOVA model based on first principles for a multi-station assembly system, as presented above in Secs. 2 and 3.1–3.4, is lengthy, tedious, and prone to error.** Relying on existing simulation-based software, an automatic SOVA model generation approach is developed below to surmount this difficulty.

The coefficients of the first-order Taylor series expansion of an assembly model can be generated by any numerical simulation based algorithm in current standard industrial software for variation analysis such as 3DCS. We take 3DCS as an example to illustrate the method for SOVA model generation. The GeoFactor in 3DCS represents the linear relationship between input and output. To automatically generate the SOVA model, we first build the 3DCS model according to assembly station sequence. At each station, we define input tolerances and RPs (as measurement points) for all parts. We then run GeoFactor station by station and record the GeoFactors of each station in matrices $\gamma_{ij}(j=1-i)$. Equation (33) can be expressed as

$$\begin{bmatrix} X(1) \\ X(2) \\ \vdots \\ X(N) \end{bmatrix} = \begin{bmatrix} \bar{\gamma}_{11} & 0 & 0 & 0 & 0 \\ \bar{\gamma}_{21} & \bar{\gamma}_{22} & 0 & 0 & 0 \\ \vdots & \vdots & \ddots & 0 & 0 \\ \vdots & \vdots & \vdots & \ddots & 0 \\ \bar{\gamma}_{N1} & \bar{\gamma}_{N2} & \cdots & \cdots & \bar{\gamma}_{NN} \end{bmatrix} \begin{bmatrix} U(1) \\ U(2) \\ \vdots \\ U(N) \end{bmatrix} = \begin{bmatrix} \gamma_{ij} \\ 0_{6(n_t-k_i)u_i} \end{bmatrix} \begin{bmatrix} U(1) \\ U(2) \\ \vdots \\ U(N) \end{bmatrix} \quad (73)$$

where n_t is the total number of parts in final product after station N , K_i is the total number of parts assembled from station 1 to i , and u_i is the total number of inputs from station 1 up to station i .

In Eq. (73), matrices $\gamma_{ij}(j=1-i)$ are constructed directly from GeoFactors in station i . Adapting state transition matrix $\Phi(\cdot, \cdot)$ from linear control theory, the state vector-input relationship can be represented as

$$X(i) = \sum_{j=1}^i \Phi(i, j)B(j)U(j) + \Phi(N, 0)X(0) \quad (74)$$

Equation (74) then becomes

$$\begin{bmatrix} X(1) \\ X(2) \\ \vdots \\ X(N) \end{bmatrix} = \begin{bmatrix} B(1) & 0 & 0 & 0 & 0 \\ A(1)B(1) & B(2) & 0 & 0 & 0 \\ A(2)A(1)B(1) & A(2)B(2) & B(3) & 0 & 0 \\ \vdots & \vdots & \vdots & \ddots & 0 \\ A(N-1) \cdots A(1)B(1) & A(N-1) \cdots A(2)B(2) & \cdots & \cdots & B(N) \end{bmatrix} \begin{bmatrix} U(1) \\ U(2) \\ \vdots \\ U(N) \end{bmatrix}$$

or

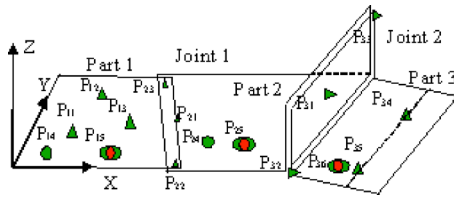


Fig. 6 Case study for validation

$$\mathbf{X} = \Psi \mathbf{U} \quad (75)$$

where, $\mathbf{X} = [X'(1), \dots, X'(N)]'$, $\mathbf{U} = [U'(1), \dots, U'(M)]'$ and

$$\Psi = [a_{ij}] \quad a_{ij} = \prod_{k=1}^{i-1} A(k) \times B(j) \quad i \geq j \quad a_{ij} = 0 \text{ otherwise}$$

A method is developed to automatically generate the SOVA model based on a simulation based method. A standardized industrial software platform (e.g., 3DCS), which is a MC based simulation tool for 3D rigid assemblies, can be used for SOVA model generation. Once the SOVA model is created, the entire subsequent forward and backward analyses can be conducted based on this linear model efficiently.

Comparing Eqs. (73) and (75), we get

$$\begin{aligned} B(1) &= \bar{\gamma}_{11} \\ A(1) &= \bar{\gamma}_{21} \bar{\gamma}_{11}^{-1} & B(2) &= \bar{\gamma}_{22} \\ A(2) &= \bar{\gamma}_{31} \bar{\gamma}_{21}^{-1} & B(3) &= \bar{\gamma}_{33} \\ &\vdots & & \\ A(N) &= \bar{\gamma}_{N1} \bar{\gamma}_{(N-1)1}^{-1} & B(3) &= \bar{\gamma}_{NN} \end{aligned} \quad (76)$$

The linear model of observed variables key product characteristics (KPCs) and variation sources in Eqs. (66) and (69) can also be obtained in the same way. This model allows for backward applications in design synthesis and diagnosis.

The process of automatic model generation is to use the numerical simulation to transform a nonlinear assembly model into an explicit linear SOVA model. It requires only a few runs of simulation. Once the model is created, all the subsequent applications, which are usually very computation intensive with simulation techniques, are conducted by using the generated SOVA model. Therefore, it can greatly enhance the applicability of SOVA model for complex assemblies. It allows for seamless integration of current numerical simulation algorithms such as 3DCS and SOVA modeling techniques. The latter can be developed as an "add on" module and embedded in existing software.

4 Model Validation

Three cases were designed for model validation. The first case was to compare the developed 3D SOVA model with MC simulation on the model without linearization, which was taken as a benchmark. The second and third cases used a floor-pan assembly and a real automotive body assembly. The comparisons were made between the SOVA models and standardized industrial software (3DCS).

Case I. A three-part assembly is designed for validation purposes. The assembly is shown in Fig. 6 with three parts assembled in three stations. The assembly sequence and datum shift scheme are shown in Fig. 7. The error sources are fixture errors and mat-

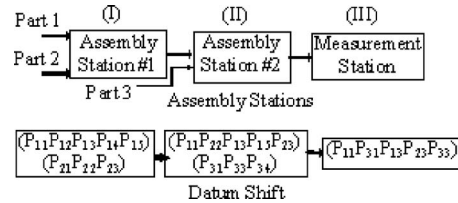


Fig. 7 PLP layout and shift schemes

ing feature planes' error. The fixture errors are assumed following normal distribution $N(0, 0.5)$. The translation error components of mating features are also assumed following $N(0, 0.5)$. Rotational error components of these features are assumed following $N(0, (5\pi/180)/6)$; i.e., the tolerance range for rotations will be limited within ± 2.5 deg. For the sake of simplicity, all data points are in one plane $Z=0$. There are two mating feature planes. The first one is lap joint with 30 deg rotation with respect to the Z axis, and the second one is butt joint with -15 deg rotation with respect to the Z axis. Since fixture deviations at the measurement station are substantially smaller, they could be regarded as zero. The state space model is built up to represent error propagation in multi-station assembly. The design nominal dimension for fixture locator part locating points (PLPs) and measurement locating points (MLPs) are given in Tables 2 and 3, respectively.

MC simulation is based on the complete model without any linear approximation and the run number is set as 10,000. All the coordinates of locators and RPs on features are given in Tables 2–4, respectively. The standard deviations of measurement points (MLP_k , $k=1-4$) on all parts are shown in Table 2. The relative error is defined as $100\% \times |\sigma_{MC} - \sigma_{SOVA}| / \sigma_{MC}$. All relative errors $< 1\%$, this accuracy is satisfactory. The total time spent on MC in this case study is 132.06 s, most of the time is spent on random number generation and the associated calculations, while the SOVA model took only 0.11 s, i.e., 0.0833% of the time used by MC.

Case II. Case II is a floor-pan assembly with four parts assembled in three stations, as shown in Fig. 8. This subassembly is used on an underbody of an automotive body assembly. The points, straight lines, and triangles in Fig. 8, which represent either true fixture locating points or virtual fixture locating points [14], are used for locating parts. On each part, a RP is selected as a KPC point. Using the approach presented in Sec. 3.5, the SOVA model is automatically generated through 3DCS. Defining similar error input, the SOVA model and a 3DCS model have been established and analyzed. The same relative errors were defined for comparison. The results are presented in Fig. 9. The maximum relative error is about 5–6%.

Case III. A truck cab assembly produced by one of the major domestic automobile manufacturing companies in the U.S. was used for model validation. The assembly system has 42 stations, 111 assembly operations, 1169 KCCs (tolerances), and 390 KPCs (measurement points). The SOVA model was constructed by the automatic model generation method developed in Sec. 3.5. In the modeling processes, the identical KPC and KCC points were assigned, and the 3DCS Analyst software was used to generate SOVA model matrices in Eqs. (73) and (76).

Comparison was made between all the calculated KPCs out of 3DCS Analyst and the SOVA model with the same input KCCs.

Table 2 Coordinates of PLPs (Units:cm)

P_{11}	P_{12}	P_{13}	P_{14}	P_{15}	P_{21}	P_{22}	P_{23}	P_{31}	P_{33}	P_{34}
(5,5)	(25,5)	(10,15)	(15,25)	(30,10)	(45,10)	(55,15)	(55,40)	(70,20)	(90,10)	(90,40)

Table 3 Coordinates of MLPs (Units:cm)

MLP	MLP ₁	MLP ₂	MLP ₃	MLP ₄
(X,Y,Z)	(20,20)	(40,20)	(50,30)	(80,10)

The inputs were composed of all the KCC tolerances obtained from the product design. Normal distributions of all the dimensions were assumed in the simulation. The maximum relative error of all the variances of the KPCs was 5.7% and about 99% of KPCs had the relative errors less than 3%, as shown in Fig. 10.

Once the SOVA model was generated, as a contrast to MC simulation based techniques, very high computation efficiency was achieved in tolerance analysis, since the covariance analysis in the SOVA model involved only simple matrix manipulations. This makes it particularly useful when multiple tolerance designs need to be evaluated or in tolerance synthesis in which a large number of tolerance analyses is required in optimization iterations.

5 Conclusions and Future Work

A 3D rigid assembly modeling technique is developed for stream of variation analysis (SOVA) in multi-station processes. The assembly process is modeled as a spatially indexed state space model which takes into account product and process factors such as: part-to-fixture, part-to-part, and inter-station interactions. These interactions represent the influences coming from both tooling errors and part errors. The incorporation of *generalized fixture* concept and inter-station interaction leads to the generic, unified SOVA model.

Table 4 Coordinates of mating feature RPs. (Units:cm)

M	M ₁	M ₂	M ₃
(X,Y,Z)	(40,0)	(60,10)	(100,0)

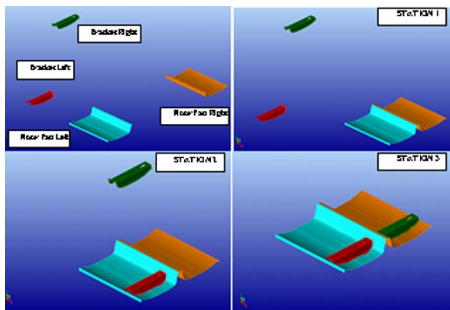


Fig. 8 Floor-pan assembly in three assembly stations

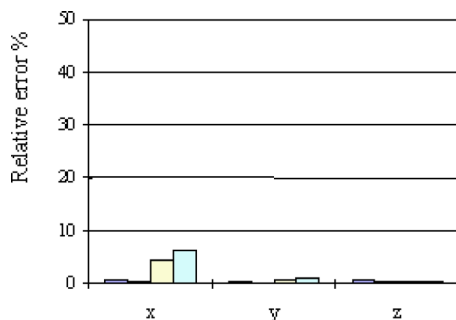


Fig. 9 Relative error comparison SOVA versus 3DCS

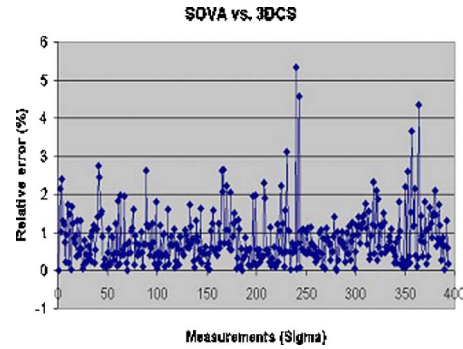


Fig. 10 Relative errors in ND33 truck cab assembly analysis (3DCS versus SOVA)

An automatic model generation technique is developed for surmounting difficulties in direct model creation based on first principles. It has been validated by case studies in this paper and industrial cases. It greatly enhances the applicability in modeling complex assemblies.

The proposed model can be used for variation control in complex assemblies such as the products in the automotive, aerospace, and shipbuilding industries. This model allows for forward and backward application which includes variation prediction, design evaluation, tolerance analysis and synthesis, system optimization, and fault diagnosis. For forward application, product variation can be predicted and the sensitivity indices at different levels such as component, station, and system levels can be defined and evaluated for design evaluation and improvement. For backward application, the model provides a linear causality relationship between variation sources and observations, which can enhance the capability for diagnosis and design synthesis. Monte Carlo based simulation, in contrast, requires a large number of runs and thus can make the backward analysis computationally intractable. In comparison, the developed model is very computationally efficient, in particular for backward applications, thus makes it possible for complex system tolerance synthesis, design optimization, and diagnosis. Some of the latest works in these applications can be found in [8,15].

Acknowledgment

The authors gratefully acknowledge the financial support of the Advanced Technology Program (ATP) award provided by the National Institute of Standards and Technology (NIST). The authors would also like to thank Dr. Z. Ying, Mr. K. Ramesh, and Mr. G. Suren of DCS Inc. for their enthusiastic support and insightful discussions.

Nomenclature

- ΔP_{ri} = the deviation of reference point on part i
- $\Delta x_i, \Delta y_i, \Delta z_i$ = deviations of locator i
- $\Delta \alpha, \Delta \beta, \Delta \gamma$ = angular deviations of a part
- \bar{F}_s = inverse of locator matrix
- \bar{J}_i = homogeneous transformation matrix for part i
- Λ = aggregated homogeneous transformation matrix
- $\bar{\Delta}$ = error source input matrix
- $\Delta \Omega_{ji}$ = feature j deviation on part i
- Δf = fixture locator deviation
- Φ = local-global coordinate transformation matrix
- $X^J(i)$ = state (deviations) vector at station i
- $E_1^J(i)$ = part/fixture induced variation vector at station i

$E_2^J(i)$ = reorientation induced variation vector at station i
 $\bar{Q}(P_{s1}(i), P_r^J)$ = point-to-point homogeneous transformation
 $A(i)$ = transformation matrix for reorientation induced variations
 $B(i)$ = transformation matrix
 $C(i)$ = observation matrix
 $P(i)$ = local variation vector
 $Y(i)$ = observation vector at station i
 $U(i)$ = deviation from local variation source at station i
 $V(i)$ = measurement noise
 $W(i)$ = unmodeled noise
 $S(i)$ = selecting matrix
 $\bar{W}_i(i=0, 1, \dots)$ = transformation matrix for part-to-part variation propagation
 $\Phi(N, i)$ = state transition matrix (from station i to station N)
 Σ_x, Σ_y = covariance matrices of x and Y

References

- [1] Ceglarek, D., and Shi, J., 1995, "Dimensional Variation Reduction for Automotive Body Assembly," *Manuf. Rev.*, **8**(2), pp. 139–154.
- [2] Hu, S., and Wu, S. M., 1992, "Identifying Root Causes of Variation in Automobile Body Assembly Using Principal Component Analysis," *Trans. NAMRI/SME*, **XX**, pp. 311–316.
- [3] Apley, D. W., and Shi, J., 1998, "Diagnosis of Multiple Fixture Faults in Panel Assembly," *ASME J. Manuf. Sci. Eng.*, **120**(4), pp. 793–801.
- [4] Ding, Y., Ceglarek, D., and Shi, J., 2002, "Design Evaluation of Multi-Station Manufacturing Processes by Using State Space Approach," *ASME J. Mech. Des.*, **124**(4), pp. 408–418.
- [5] Shiu, B. W., Apley, D., Ceglarek, D., and Shi, J., 2003, "Tolerance Allocation for Sheet Metal Assembly Using Beam-Based Model," *IIE Trans.*, **35**(4), pp. 329–342.
- [6] Ceglarek, D., Huang, W., Zhou, S., Ding, Y., Ramesh, K., and Zhou, Y., 2004, "Time-Based Competition in Manufacturing: Stream-of-Variation Analysis (SOVA) Methodology—Review," *Int. J. Flexible Manufact. System*, **16**(1), pp. 11–44.
- [7] Camelio, J. A., and Hu, S. J., 2004, "Multiple Fault Diagnosis for Sheet Metal Fixtures Using Designated Component Analysis," *ASME J. Manuf. Sci. Eng.*, **126**(1), pp. 91–97.
- [8] Kong, Z., Ceglarek, D., and Huang, W., 2007, "Multiple Fault Diagnosis Method in Multi-Station Assembly Processes Using Orthogonal Diagonalization Analysis," *Proceedings of 2005 ASME International Mechanical Engineering Congress and Exposition*, Orlando, Florida, November 5–11; *ASME Trans. J. of Manuf. Sci. Eng.*, accepted.
- [9] Huang, W., and Ceglarek, D., 2002, "Mode-Based Decomposition of Part Form Error by Discrete-Cosine-Accepted Transform With Implementation to Assembly and Stamping System With Compliant Parts," *CIRP Ann.*, **51**(1), pp. 21–26.
- [10] Huang, W., 2004, "Methodologies for Modeling and Analysis of Stream-of-Variation (SOVA) in Compliant and Rigid Assembly," Ph.D. thesis, University of Wisconsin-Madison, WI.
- [11] Huang, W., Ceglarek, D., and Zhou, Z. G., 2004, "Using Number-Theoretical Net Method (NT-Net) in Tolerance Analysis," *Int. J. Flexible Manufact. Systems*, **6**(1), pp. 65–90.
- [12] Huang, W., and Ceglarek, D., 2005, "Model Complexity Reduction in Stream of Variation for Compliant Sheet Metal Assembly," 9th CIRP Int. Seminar on Computer Aided Tolerancing, Arizona, April, 11–12.
- [13] Huang, W., and Ceglarek, D., 2005, "Statistical Modal Analysis Methodology for Form Error Modeling," revised, *IIE Trans., Quality & Reliability Engineering*, submitted.
- [14] Huang, W., Lin, J., Bezdecny, M., Kong, Z., and Ceglarek, D., 2007, "Stream-Of-Variation Modeling I: A Generic 3D Variation Model for Rigid Body Assembly in Single Station Assembly Processes," by in *Proc. of 2006 ASME MSEC; ASME Trans., Journal of Manufacturing Science and Engineering*, in press.
- [15] Huang, W., Phoomboplab, T., and Ceglarek, D., 2006, "Explicit Yield Model (EYM) for Tolerance Synthesis of Large Scale Complex Assemblies," *Proceedings of ASME MESC2006*, Paper No. MSEC2006-21074.
- [16] Shalon, D., Gossard, D., Ulrich, K., and Fitzpatrick, D., 1992, "Representing Geometric Variations in Complex Structural Assemblies on CAD Systems," *ASME Advances in Design Automation*, 18th Annual ASME Design Automation Conference, Scottsdale, AZ, Vol. 2, pp. 121–132.
- [17] Shiu, B. W., Ceglarek, D., and Shi, J., 1996, "Multi-Stations Sheet Metal Assembly Modeling and Diagnostics," *Trans. NAMRI/SME*, Vol. **XXIV**, pp. 199–204.
- [18] Jin, J., and Shi, J., 1999, "State Space Modeling of Sheet Metal Assembly for Dimensional Control," *ASME J. Manuf. Sci. Eng.*, **121**, pp. 756–762.
- [19] Mantripragada, R., and Whitney, D. E., 1999, "Modeling and Controlling Variation Propagation in Mechanical Assemblies Using State Transition Models," *IEEE Trans. Rob. Autom.*, **15**(1), pp. 124–140.
- [20] Ceglarek, D., Shi, J., and Wu, S. M., 1994, "A Knowledge-Based Diagnostic Approach for the Launch of the Autobody Assembly Process," *ASME J. Eng. Ind.*, **116**(4), pp. 491–499.
- [21] Rong, Q., Ceglarek, D., and Shi, J., 2000, "Dimensional Fault Diagnosis for Compliant Beam Structure Assemblies," *ASME J. Manuf. Sci. Eng.*, **122**(4), pp. 773–780.
- [22] Rong, Q., Shi, J., and Ceglarek, D., 2001, "Adjusted Least Squares Approach for Diagnosis of Compliant Assemblies in the Presence of Ill-Conditioned Problems," *ASME J. Manuf. Sci. Eng.*, **123**(3), pp. 453–461.
- [23] Fong, D. Y. T., and Lawless, J. F., 1998, "The Analysis of Process Variation Transmission With Multivariate Measurements," *Stat. Sin.*, **8**, pp. 151–164.
- [24] Lawless, J. F., Mackay, R. J., and Robinson, J. A., 1999, "Analysis of Variation Transmission in Manufacturing Processes—Part I," *J. Quality Technol.*, **31**(2), pp. 131–142.
- [25] Agrawal, R., Lawless, J. F., and Mackay, R. J., 1999, "Analysis of Variation Transmission in Manufacturing Processes—Part II," *J. Quality Technol.*, **31**(2), pp. 143–154.
- [26] Zhou, Z., Huang, W., and Zhang, L., 2001, "Sequential Algorithm Based on Number Theoretic Method for Statistical Tolerance Analysis and Synthesis," *ASME J. Manuf. Sci. Eng.*, **123**(3), pp. 490–493.
- [27] Shiu, B. W., Ceglarek, D., and Shi, J., 1997, "Flexible Beam-Based Modeling of Sheet Metal Assembly for Dimensional Control," *Trans. NAMRI/SME*, Vol. **25**, pp. 49–54.
- [28] Shi, J., 2006, "Stream of Variation Modeling and Analysis for Multistage Manufacturing Processes," CRC Press, Boca Raton, FL.